applied optics

Validation of a gonio-hyperspectral imaging system based on light-emitting diodes for the spectral and colorimetric analysis of automotive coatings

Francisco J. Burgos-Fernández,[1,*] Meritxell Vilaseca,[1] Esther Perales,[2] Elísabet Chorro,[2] Francisco M. Martínez-Verdú,[2] José Fernández-Dorado,[1] and Jaume Pujol[1]

[1]Centre for Sensors, Instruments and Systems Development, Polytechnic University of Catalonia, Rambla Sant Nebridi 10, Terrassa 08222, Spain
[2]Department of Optics, Pharmacology and Anatomy, University of Alicante, San Vicente del Raspeig Road, San Vicente del Raspeig 03690, Spain
*Corresponding author: francisco.javier.burgos@upc.edu

Received 26 May 2017; revised 2 August 2017; accepted 7 August 2017; posted 7 August 2017 (Doc. ID 296812); published 29 August 2017

In this study, a novel gonio-hyperspectral imaging system based on light-emitting diodes for the analysis of automotive coatings was validated colorimetrically and spectrally from 368 to 1309 nm. A total of 30 pearlescent, 30 metallic, and 30 solid real automotive coatings were evaluated with this system, the BYK-mac and X-Rite MA98 gonio-spectrophotometers, and also with the SPECTRO 320 spectrometer for further comparison. The results showed very precise correlations, especially in the visible range. In conclusion, this new system provides a deeper assessment of goniochromatic pigments than current approaches due to the expansion of the spectral range to the infrared.

OCIS codes: (010.1690) Color; (110.4234) Multispectral and hyperspectral imaging; (230.3670) Light-emitting diodes; (160.4760) Optical properties.

https://doi.org/10.1364/AO.56.007194

1. INTRODUCTION

Goniochromatic pigments, also called effect or gonioapparent pigments, are known by their appearance changes as a function of the angles of illumination and observation [1–3]. These changes can affect both color and texture, resulting in very diverse visual impressions. Accordingly, they are classified as pearlescent pigments, which mainly exhibit hue and chroma shifts, and metallic pigments, which show lightness variations; the traditional absorption pigments with a constant angular appearance are designated as solids. These pigments have acquired relevance in the industry during the last two decades, specifically in the automotive, cosmetic, printing, and packaging sectors [2,4].

The angle-dependent coatings prompted the definition of a new angular concept, the aspecular angle, which corresponds to the angle between the specular reflection and the direction of observation. Two additional concepts, the interference and aspecular lines, were subsequently generated (Fig. 1). These lines are used in the representation of the visual appearance of goniochromatic samples in a color space. The aspecular angle remains constant along the interference line, while the illumination angle is variable. However, in the aspecular line the illumination angle remains invariable. The main function of the interference line is to reveal abrupt shifts in hue and chroma for different illumination angles (pearlescent pigments), in contrast to the aspecular line, where lightness shows the most significant variation when moving far away from the specular reflection (metallic pigments).

The growing use of coatings based on goniochromatic pigments called for the characterization at different illumination and observation geometries. Since traditional devices included just one fixed configuration, the multi-angle or gonio-spectrophotometers were created to provide more accurate assessments of effect pigments through a larger variety of measurement geometries [5]. At the same time, new standards for the complete evaluation of these pigments were issued by the German Institute for Normalization (Deutsches Institut für Normung, DIN) and the American Society for Testing Materials (ASTM) [6–8]. First, the guidelines for the analysis of metallic pigments were detailed in DIN 6175-02 and ASTM E2194. The measurement geometries described the fixed angle of illumination for the correct assessment of lightness variations along the observations angles. Since these two standards could not accurately characterize pearlescent pigments, a specific standard, ASTM E2539, was later issued. This new standard recommends two illumination angles since chroma and hue

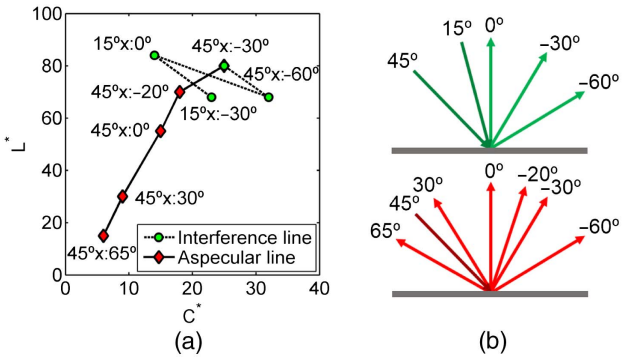

Fig. 1. Interference and aspecular lines: (a) C^* and L^* diagram showing the behavior along the different measurement geometries. (b) Measurement geometries for the interference (top) and aspecular lines (bottom).

shifts of pearlescent pigments mostly appear for different directions of illumination. Table 1 summarizes the measurement geometries recommended by these three standards.

In addition, values were established for the aperture angle (2σ) between the sample and the illumination and observation directions, defined as the angle subtended by the sensor or the light source with respect to the center of the sample. For ASTM E2194 and ASTM E2539, the angle should be $2\sigma < 8°$ and equal for both directions, while DIN 6175-2 specifies the value of these angles for each measurement geometry. Furthermore, this standard differentiates between constant and variable directions, which can refer to the illumination or observation beams, depending on which has the fixed element. Therefore, the aperture angle for the constant direction must be $2\sigma \leq 5°$ and for variable directions $2\sigma_{-20°} \leq 4°$, $2\sigma_0 \leq 4°$, $2\sigma_{30} \leq 10°$, and $2\sigma_{65} \leq 10°$. Another condition is the CIE 1964 standard observer (10°) proposed by the Commission Internationale del'Éclairage (CIE). The colorimetric features of goniochromatic pigments require a large field of view evaluation due to the broad spatial distribution of pearlescent and metallic particles over the sample.

In view of these developments, all large companies involved in color measurement (Datacolor, Konica Minolta, GretagMacbeth, X-Rite, BYK Additives & Instruments, Hunterlab, etc.) have launched desktop or portable gonio-spectrophotometers. The major driving force has been the interest of the automotive industry in improving the visual quality control of car finishes. Indeed, the automotive industry is still the sector with a stronger demand for goniometric analysis.

Table 1. Measurement Geometries of DIN 6175-02, ASTM E2194, and ASTM E2539 Standards[a]

Standards	Measurement Geometries			
DIN 6175-02, ASTMs	45° × : -20°	45° × :0°	45° × :30°	45° × :65°
ASTM E2194, E2539	45° × : -30°			
ASTM E2539	45° × : -60°	15° × :0°	15° × : -30°	

[a]Angle of illumination with respect to the normal; x: angle of observation with respect to the normal.

Experimental gonio-spectrophotometers have also been developed with diverse operating principles and providing additional parameters: gonio-spectro-photometry based on the spectral bidirectional reflectance distribution function (sBRDF) [9,10], direct measure of the gloss at various geometries [11,12], and versatile optomechanical designs for measurements at several geometries [13]. Despite the good performance of commercial and experimental gonio-spectrophotometers, the data generally result from integrating the information of a few square millimeters of the target object. Consequently, they lack spatial resolution. For this reason, these devices can be considered to not properly estimate perceptual aspects of a surface as psychophysical experiments with real observers. At this point, the combination in hyperspectral imaging of colorimetric and textural assessments required for the special visual attributes of these coatings was considered to be the best approach to overcome these constraints.

The combination of gonio-spectrophotometers and spectral imaging systems has generated a new kind of instruments known as gonio-spectral imaging systems or multi-angle spectral imaging systems, with the main objective to obtain spectral images at different geometries. The first approaches to gonio-spectral imagery focused on the analysis of three-dimensional pieces of artwork [14–16], and later extended to two-dimensional objects such as paper and cloth samples [17,18]. The illumination system consisted of a wide spectrum light source and sets of interference filters resulting in a large and mechanically complex structure. However, it is now possible to obtain the spectral sampling directly from the light source without added elements by means of light-emitting diodes (LEDs). The advantages of LEDs are widely known: they are very efficient, present a long life cycle, evolve constantly, are comparatively economical, and have a small size. In addition, these diodes have a narrow spectral emission, and they are available at several wavelength peaks along different spectral ranges (ultraviolet, UV; visible, VIS; and infrared, IR). Another relevant advantage of LED technology is the modulation of their emission as a function of the forward current.

In the existing literature, goniochromatic pigments have only been evaluated in the VIS range of the electromagnetic spectrum, since it is the region where the main appearance shifts occur [19–21]. However, an analysis of the angular dependence at deeper layers through IR illumination would further elucidate the behavior of these pigments. Furthermore, ultraviolet lighting can contribute to a better insight into possible fluorescence. Thus, an extended spectral inspection might provide valuable information on the performance of these coatings in a broad range of bands of the electromagnetic spectrum.

This paper presents the validation of GOHYLED, a new gonio-hyperspectral imaging system based on LEDs, developed for the spectral and colorimetric evaluation of automotive coatings. This initial verification will establish the basis for future work on spatially resolved assessments. GOHYLED is specifically intended to work in an extended range from the UV to IR by using commercial, high power LEDs, in contrast

with conventional gonio-spectral systems that only use wide spectrum light sources that exclusively cover the VIS range.

2. EXPERIMENTAL SETUP

The experimental setup was based on the requirements for the study of automotive coatings in a wide spectral and angular range specified by the DIN 6175-2, ASTM E2194-09, and ASTM E2539-08 standards [6–8]. However, it might be useful for other applications and configurations. Essentially, the GOHYLED is composed of a spectral light source, two cameras (UV-VIS and IR) that cover the 368–1309 nm range, and two rotation stages with a total rotation angle of 180° in both observation and illumination directions (Fig. 2). All elements were controlled through a purpose-built graphical user interface developed with MATLAB R2013a, which allows the individual and synchronized use of the light source, cameras, and motorized rotation stages.

A. Light Source

The light source consists of 28 high power surface-mounted-device (SMD) LED clusters of different peak wavelengths that spectrally illuminate the sample and a linear actuator that sequentially positions each cluster in front of it. A white

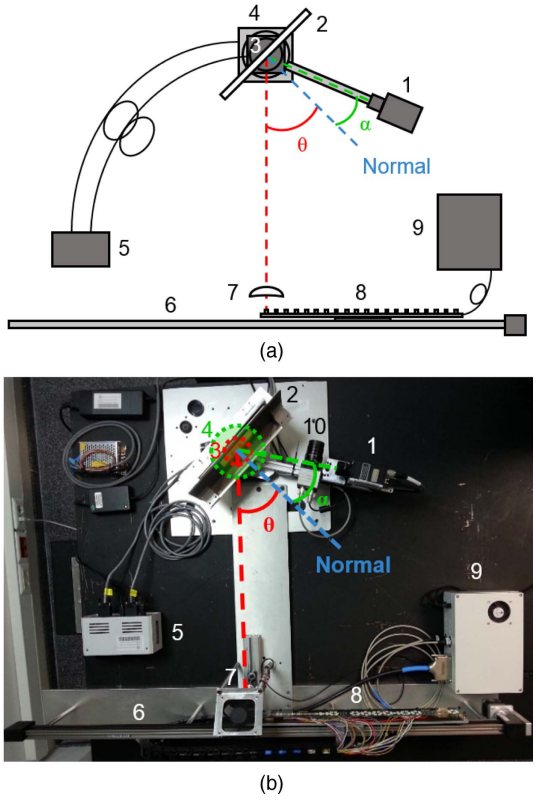

Fig. 2. Developed gonio-hyperspectral imaging system based on LEDs represented in (a) a layout and in (b) a picture: 1, UV-VIS camera; 2, sample holder; 3, 8MR191-30 rotation stage; 4, 8MR191-30-28 rotation stage; 5, rotation stages controller; 6, linear actuator; 7, lens; 8, LED clusters; 9, light source controller and power supply; 10, IR camera, which is not represented in (a). θ refers to the illumination angle controlled by the 8MR151-30 rotation stage and α to the observation angle handled by the 8MR191-30-28 rotation stage.

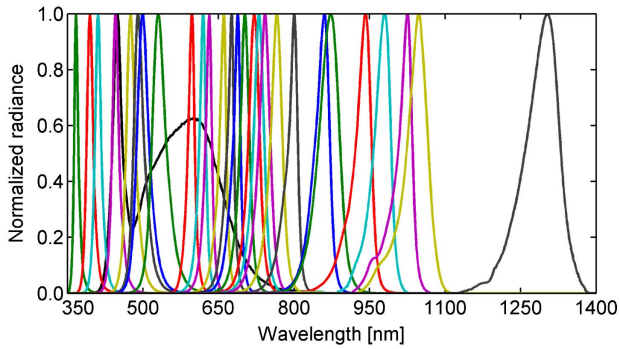

Fig. 3. Normalized spectral radiance of the LEDs included in the GOHYLED system.

LED cluster was also incorporated for the subsequent spatial evaluation of texture, which is not included in this work. The clusters are composed of three or six LEDs, depending on the radiance emitted. A lens to increase the amount of light over the sample was also incorporated. Figure 3 shows the normalized spectral radiance, and Table 2 contains the part number and peak wavelengths of the whole set of LEDs.

The LEDs were purchased from Roithner LaserTechnik GmbH (Part numbers RLCU and SMB1N) and Lumileds Holding B.V. (Part numbers LX). The UV-VIS LEDs (368–774 nm) presented a mean spectral step between consecutive peak wavelengths of around 20 nm, whereas in the IR (807–1309 nm), this value increased to 40 nm. The FWHM in the UV-VIS range varies from 10 to 37 nm and from 30 to 80 nm in the IR. The higher FWHM and the subsequent overlapping of the spectra in the IR range partially compensated the larger distance among peak wavelengths. Even though it causes a coarser sampling, the broader FWHM is a typical feature of current IR solid-state technology that is still unsolved. Moreover, IR LEDs present less variety of wavelengths, especially those of high power—thus the significant gap before the spectrum with a peak wavelength of 1309 nm in Fig. 3.

Table 2. Part Numbers and Peak Wavelengths (λ_p) of the 28 Types of LEDs

Part Number	λ_p [nm]	Part Number	λ_p [nm]
RLCU-440-365	368	SMB1N-700	709
RLCU-440-390	397	RLCU-440-720	724
RLCU-440-410	411	SMB1N-735	735
LXML-PR01-0500	446	SMB1N-750	748
LXML-PB01-0040	476	SMB1N-770	774
SMB1N-490	489	SMB1N-810D	807
LXML-PE01-0070	498	SMB1N-850D	867
LXML-PM01-0100	528	SMB1N-870	885
LXML-PL01-0060	601	SMB1N-940D	952
LXM2-PH01-0070	622	RLCU-440-970	984
LXM2-PD01-0050	634	RLCU-440-1020	1033
LXM3-PD01	663	RLCU-440-1050	1052
SMB1N-670D	678	SMB1N-1300	1309
SMB1N-690D	693	LXW8-PW40	449/599[a]

[a]Peak wavelengths of the two peaks for the white LEDs.

The use of high power LEDs was driven by the aperture angles recommended by the standards. To achieve such small angles, the illuminating and sensing areas should have been extremely reduced, limiting the evaluation to a minute fraction of the samples. However, one of the objectives of this work was to evaluate bigger areas than current devices and to obtain spatially resolved images. To this end, the LEDs were placed at a distance of 580 mm in order to leave enough free space for the rotation of the acquisition arm around the sample. But the long distance and the angle of emission of the LEDs (120°) resulted in a low illumination of the sample. To solve this issue, a plano-convex lens from Edmund Optics (stock #67-228) with a focal length of 75 mm, a diameter of 50 mm, and a transmittance of 90% from 200 to 1300 nm was selected. The relative position between the LEDs and the lens was out of focus to avoid an image of the LED chips to form on the sample. The lens back surface was finally placed 25 mm from the LEDs; this was experimentally determined and ensured a uniform illumination over the sample. This configuration of the light source produced an aperture angle of 4.69°, which was below the maximum tolerance of the ASTM E2194 and E2539 (8°) and DIN 6175-2 (5°) standards, considering for the latter the illumination beam as the constant direction.

The linear actuator ZLW-0630-02-B-60-L-1000 from Igus S.L., and a stepper motor SY42STH47-1206A from Changzhou Songyang Machinery & Electronics Co., Ltd., executed the sequential positioning of the LED clusters, resulting in a minimum step of 140 μm. Each LED cluster was switched on only when it was placed in front of the sample and behind the lens. The images were then acquired by the camera, the LEDs were switched off, and the next cluster was placed in the same position to repeat the process. With this method, only one LED cluster was switched on at a time.

B. Imaging Sensors

Table 3 contains the technical features of the two cameras used. The acquisition unit included a CM-140 GE-UV monochromatic CCD camera from JAI AS, with enhanced UV sensitivity, and a GMUV42528C 2.8/25 mm quartz lens from GOYO OPTICAL Inc. selected specifically for its high transmittance from 200 to 1300 nm. The InGaAs camera was a Hamamatsu C10633-23 with a lower spatial resolution and exposure time and no available gain factor. A Kowa LM12HC-SW 1.4/12.5 mm SWIR lens with high transmission from 800 to 2000 nm was coupled to this camera. The spatial resolution of the IR camera did not pose a problem since the validation of the proposed system was performed by means of averaged reflectances of the images. However, it can limit future spatial evaluations.

The acquisition was made in a two-step process. The UV-VIS camera was employed to acquire images when using the LED clusters with peak wavelengths from 368 to 952 nm, and the IR camera for peak wavelengths from 984 to 1309 nm. The images for the whole set of measurement geometries were first captured with the UV-VIS and second with the IR camera.

Table 3. Technical Features of the Cameras

Camera	UV-VIS	IR
Spectral range [nm]	200–1000	900–1650
Sensor size [px]	1392 × 1040	320 × 256
Bit depth	10	14

The aperture angles of the observation stage also conformed to the standards. The minimum distance between the sample and the cameras was based on the maximum diameter of the entrance pupil. Since it can be obtained dividing the focal length by the minimum F-number, the lenses of both cameras presented the same value of 8.93 mm. However, the distance to the sample was different for each camera because the position of the entrance pupil was different for each lens, at 14.1 mm for the UV-VIS lens and at 10.7 mm for the IR lens, both inward. Consequently, the minimum distances between the sample and the outer part of the cameras' lenses were 113.8 mm for the UV-VIS and 117.1 mm for the IR. Finally, the UV-VIS camera was positioned at 218 mm from the sample to increase the area observed; this resulted in one aperture angle of 2.20°. The IR camera was located at 129 mm from the sample to avoid any collision with the sample holder; this distance variation generates an aperture angle of 3.66°. A longer distance was not used for this camera because of its wider field of view and lower spatial resolution. Both cameras conformed to the tolerance of the ASTM E2194 and E2539 (8°) and DIN 6175-2 (4°) standards, considering for the latter the observation beam as the variable direction. Although these standards only regulate the measurement of goniochromatic pigments in the VIS range, the same conditions were applied to the IR due to the lack of regulations in this range.

To capture images within the dynamic range of the cameras, exposure time and gain varied throughout the measurement geometries and for the different acquisition channels. Besides the emission power of each LED cluster, the spectral sensitivity of the cameras and the angular distance between the illumination and observation direction also conditioned these parameters.

C. Motorized Rotation Stages

The changeable angular positioning was obtained using two motorized rotation stages manufactured by STANDA Ltd, the 8MR151-30 and the 8MR191-30-28. Both have a rotation range of 360°, an angular resolution of 0.01°, and a central aperture of 30 mm. At the top, the 8MR151-30 stage controls the illumination angle by rotating the sample, while at the bottom, the 8MR191-30-28 controls the observation direction by positioning the cameras around the sample. Figure 2 shows a graphical description of the angular positioning of each stage.

3. METHODS

A. Samples

A total of 30 pearlescent, 30 metallic, and 30 solid samples were selected; they presented a rectangular size between 90 mm × 150 mm and 100 mm × 200 mm. The 90 samples originated from AUDI AG, BASF SE, and PPG Industries Inc. commercial car paints. In addition to the measurements carried out with the GOHYLED system, these samples were measured with the BYK-mac (BYK-Gardner GmbH) and X-Rite MA98 (X-Rite Inc.) gonio-spectrophotometers and also the

SPECTRO 320 spectrometer (Instruments Systems GmbH) for further comparisons.

B. Multi-Angle Color Measurement

The GOHYLED system was designed and built considering the measurement geometries, aperture angles, and CIE standard observer recommended by the DIN 6175-2, ASTM E2194-09, and ASTM E2539-08 standards (Table 4). The aperture angle for the UV-VIS camera was eventually smaller because the diaphragm size of the camera lens was diminished ($f/11$) to enhance the focus at the 368–952 nm spectral range. In contrast, the IR camera used a greater diaphragm ($f/2.8$) to ensure a good signal-to-noise ratio, since IR LEDs had lower power than VIS LEDs. Furthermore, the focus was less critical than in the UV-VIS region because the IR camera operated with LEDs in a range of only 300 nm. The measurement area or region of interest (ROI) was determined for the UV-VIS camera because its field of view was more limited.

The major benefit of conforming to ASTM and DIN specifications is the possibility of performing a precise comparison of readings among instruments of different optical design. The measurements obtained with the GOHYLED system were compared to those of the BYK-mac and X-Rite MA98 gonio-spectrophotometers. These devices are calibrated for all the geometries against ceramic standards of the British Ceramic Research Association, known as BCRA tiles. The BYK-mac conforms only to the DIN 6175-2 and ASTM E2194 standards, whereas the X-Rite MA98 and the GOHYLED conform to the three standards (DIN 6175-2, ASTM E2194, and ASTM E2539). With a fixed illumination direction, the BYK-mac is particularly suitable for the evaluation of metallic pigments, but it cannot characterize the changes of hue and chroma that appear in pearlescent pigments for different illumination directions. Similarly to the GOHYLED, the BYK-mac performs the spectral sampling by means of LEDs and can evaluate sparkle and graininess, both textural effects of goniochromatic pigments. On the other hand, the X-Rite MA98 can produce complete assessments of pearlescent and metallic pigments since it includes the 45° and 15° illumination angles required by the standards. It also includes other observation angles outside the conventional plane of illumination/observation, and a diffraction grating performs the spectral sampling. Besides the standard, the BYK-mac and X-Rite MA98 also perform evaluations at the 45° × : -60° measurement geometry. Therefore, the spectral and colorimetric results obtained with the GOHYLED system were fully comparable to those of the X-Rite MA98, whereas only the geometries suggested by the DIN 6175-2 and ASTM E2194 standards, 45° × : -30°, 45° × : -20°, 45° × :0°, 45° × :30°, and 45° × :65°, plus 45° × : -60°, were used to compare with the results of the BYK-mac.

Table 4. F-Number, Aperture Angles (2σ), Spatial Resolutions (SR), and Regions of Interest (ROI) for Each Camera

Camera	F-Number	2σ [°]	SR [px/mm]	ROI [mm]
UV-VIS	$f/11$	0.56	28	50 × 37
IR	$f/2.8$	1.83	3	50 × 37

C. Measurement Stability and Repeatability

The stability and repeatability of the measurement procedure were also evaluated through the acquisition of images of a white reference BN-R98-SQ10C from Gigahertz Optik GmbH at the geometry of 45° × :0° with both cameras and the quantification of the mean digital level variation.

First, the stability of all the spectral channels was examined by switching every LED cluster on and off 10 times and each time capturing 10 images, which were subsequently averaged. The purpose of these tests was to accurately reproduce the final measurement mechanism, in which the LED clusters were used as flashes of light. Next, the influence of the sample positioning on the holder was evaluated. This study encompassed the comparison of measurements with and without the replacement of the sample among repetitions.

In order to reduce other sources of bias such as temporal noise, sets of three, five, and 10 averaged frames were tested for the two cameras at the geometries of 45° × : -60°, 45° × : -30°, 45° × : -20°, 45° × :0°, 45° × :30°, and 45° × :65°, using the white reference mentioned before.

The proposed system also dealt with spatial noise removal, in this case by applying Eq. (1) to each acquired image:

$$I_C(i,j) = k\frac{I(i,j) - I_B(i,j)}{I_U(i,j) - I_B(i,j)}, \tag{1}$$

where $I_C(i,j)$, $I(i,j)$, $I_B(i,j)$, and $I_U(i,j)$ correspond to the digital levels of the corrected, raw, background or dark, and uniform field or white reference images, respectively; k is the calibrated reflectance of the reference provided by the manufacturer. $I(i,j)$, $I_B(i,j)$, and $I_U(i,j)$ images were always acquired in the same conditions of exposure time and gain, which change for each acquisition channel and measurement geometry. Images of the calibrated white reference were captured and used as uniform field targets, as well as dark or background images with all LEDs turned off. The results derived from Eq. (1) were directly expressed as reflectance images.

The evaluation of the positioning repeatability of the rotation stages was carried out by means of the UV-VIS camera attached to the 8MR191-30-28 stage through the acquisition arm at the distance previously calculated (218 mm from the sample). A graph paper divided into 1 mm squares was used as the sample to quantify the deviation of the image recorded. Positioning tests were performed for rotations of 30°, 10°, and 5°, first with one of the two elements fixed and afterwards moving both; each rotation displacement was assessed three times.

D. Extraction of Reflectance Spectra and Colorimetric Data

The spectral and color appearance data were retrieved by means of a purpose-developed image processing program using MATLAB R2013a. Its main functions were to calculate the reflectance spectra, spectral fitting metrics, chromatic coordinates, and color differences.

Reflectance images were obtained by means of Eq. (1). Throughout the whole spectral range of the GOHYLED system (368–1309 nm), the average reflectance values were also

determined for three ROIs: the ROI detailed in Table 4 and the ROIs of the BYK-mac and the X-Rite MA98 gonio-spectrophotometers with diameters of 23 and 12 mm, respectively. Although the ROIs of the GOHYLED system are square or rectangular and those of the two gonio-spectrophotometers are circular, the differences were considered negligible. These spectra were finally interpolated from 400 to 700 nm with a step of 10 nm by applying a cubic spline algorithm [22,23], on account of the input spectral range needed for calculating the colorimetric values and color differences with respect to those of the BYK-mac and X-Rite MA98. Regarding the IR range, the spectra were validated with the measurements carried out with the SPECTRO 320 spectrometer and the telescopic optical probe TOP 100 from Instrument Systems GmbH and a halogen lamp at the geometries of 45° × :30°, 45° × :0°, and 15° × :0°. This device and all its accessories are calibrated against standards of the National Institute of Standards and Technology (NIST) and the Physikalisch-Technische Bundesanstalt (PTB). The spectral range went from 700 to 1309 nm with a step of 10 nm. No additional geometries were assessed since these were considered sufficiently representative and also due to the lack of automation of the measurement process.

Additionally, the comparison of the spectra between the GOHYLED system and the BYK-mac, the X-Rite MA98, and the SPECTRO 320 was completed through the mean absolute error (MAE), root mean square error (RMSE) [24,25], and goodness-of-fit coefficient (GFC) [26,27]. These metrics were chosen because they are commonly used when comparing reconstructed spectral data [25,27,28]. Moreover, the combination of the MAE and RMSE is useful to detect whether values are caused by generalized large errors (RMSE ∼ MAE) or by a few errors greater than MAEs, such as outliers (RMSE > MAE); both parameters are in the same units as the analyzed data. On the other hand, the GFC is a relative measure between 0 and 1 based on Schwartz's inequality, commonly used when comparing spectra and, especially, color differences [Eq. (2)]. According to the scale commonly linked to this parameter [27], a GFC ≥ 0.9950 is considered "colorimetrically accurate," a GFC ≥ 0.9990 a "good spectral fitting," and a GFC ≥ 0.9999 an "excellent spectral fitting":

$$\mathrm{GFC} = \frac{\left|\sum_i^n r_o(\lambda_i) r_e(\lambda_i)\right|}{\sqrt{\sum_i^n [r_o(\lambda_i)]^2 \sum_i^n [r_e(\lambda_i)]^2}}, \tag{2}$$

where $r_o(\lambda_i)$ is the original spectrum and $r_e(\lambda_i)$ is the estimated spectrum, both evaluated at the same wavelength λ_i; n is the total amount of wavelengths considered.

The colorimetric evaluations were performed under the CIELAB color space [29,30]. The CIE standard illuminant selected was D65, similarly to BYK-mac and X-Rite MA98. Color differences between these devices and the GOHYLED were calculated with the CIEDE2000 [31,32] and AUDI2000 [33] color-difference formulas. The CIEDE2000 color-difference formula is defined as

$$\Delta E_{00} = \left[\left(\frac{\Delta L'}{k_L S_L}\right)^2 + \left(\frac{\Delta C'}{k_C S_C}\right)^2 + \left(\frac{\Delta H'}{k_H S_H}\right)^2 + R_T \left(\frac{\Delta C'}{k_C S_C}\right)\left(\frac{\Delta H'}{k_H S_H}\right)\right]^{\frac{1}{2}}, \tag{3}$$

where $\Delta L'$, $\Delta C'$, and $\Delta H'$ are differences of lightness, chroma, and hue between two colors, respectively. This formula included parametric factors k_L, k_C, and k_H for weighting lightness, chroma, and hue differences, respectively, according to the application. These three parameters are equal to 1 under the reference conditions proposed by the CIE [34,35]. In addition, three weighting functions, S_L, S_C, and S_H for each lightness, chroma, and hue, were also included. Finally, the rotation term R_T was added to improve the performance for blue colors. The improved performance for objects that exhibit lightness values higher than 100 was a decisive factor, since this phenomenon is very common in goniochromatic pigments, especially under direct illumination conditions.

On the other hand, the AUDI color-difference formula was specially developed for the approval of goniochromatic paint batches as follows:

$$dE'_\gamma = \left[\left(\frac{dL^*_\gamma}{k_{dL} s_{dL_\gamma}}\right)^2 + \left(\frac{dC^*_\gamma}{k_{dC} s_{dC_\gamma}}\right)^2 + \left(\frac{dH^*_\gamma}{k_{dH} s_{dH_\gamma}}\right)^2\right]^{\frac{1}{2}}. \tag{4}$$

The main difference with respect to the CIEDE2000 is that, in this case, the weighting functions (s_{dL_γ}, s_{dC_γ}, s_{dH_γ}) depend on the measurement geometry.

4. RESULTS AND DISCUSSION

The spectral reconstruction of the 90 samples comprised the entire spectral range of the GOHYLED system, from 368 to 1309 nm, with 28 acquisition channels, eight color measurement geometries, and three ROIs. Figure 4 shows two reflectance images of a pearlescent pigment at the geometries of 45° × : -30° and 45° × : -20° and for the LED cluster with a peak wavelength of 476 nm. The illumination gradient was not removed when dividing by the image of the white reference because it has a matte finish, whereas the automotive coatings were glossy. At this stage, a glossy white reference was not used to reach a more precise comparison with the BYK-mac and the X-Rite MA98, which also employ a matte white reference.

Figure 5 exhibits the reflectance spectra, and Fig. 6 the C^* versus L^* of three samples where the pearlescent, metallic, and solid effects were more noticeable. Measured samples showed the expected theoretical behavior that was also confirmed by the commercial devices. Chroma shifts were more evident in pearlescent samples due to variations of the reflectance spectrum in relation to wavelength and to the interference and aspecular lines. Luminance changes in goniochromatic samples

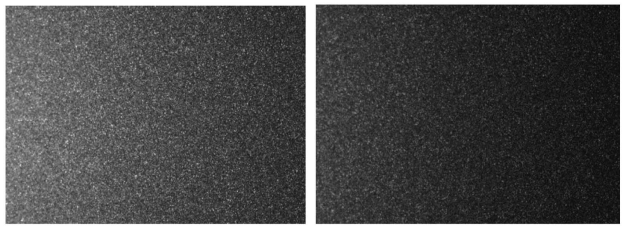

Fig. 4. Reflectance images of a pearlescent pigment at the geometries of (a) 45° × : -30° and (b) 45° × : -20° for the LED cluster with a peak wavelength of 476 nm.

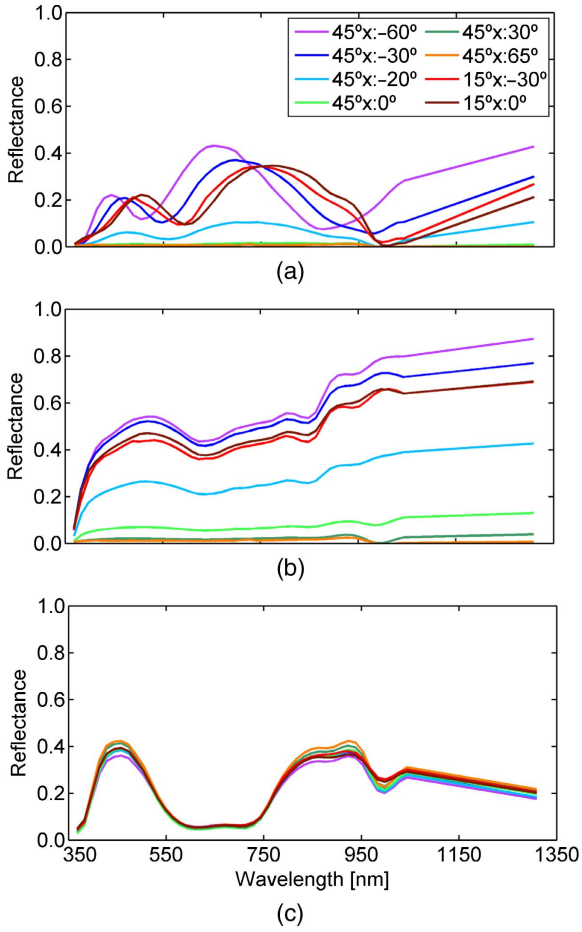

Fig. 5. Reflectance spectra of (a) pearlescent, (b) metallic, and (c) solid samples at 45° × : -60°, 45° × : -30°, 45° × : -20°, 45° × :0°, 45° × :30°, 45° × :65°, 15° × : -30°, and 15° × :0°.

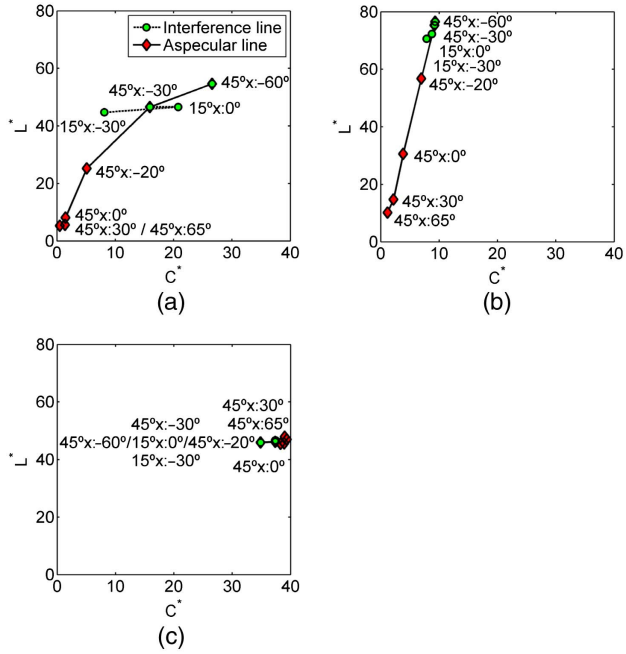

Fig. 6. C^* and L^* diagrams of (a) pearlescent, (b) metallic, and (c) solid samples at 45° × : -60°, 45° × : -30°, 45° × : -20°, 45° × :0°, 45° × :30°, 45° × :65°, 15° × : -30°, and 15° × :0°.

were recorded as variations in reflectance [Figs. 5(a) and 5(b)] and lightness [Figs. 6(a) and 6(b)]. Although this phenomenon is the main attribute of metallic samples, it was also observed in pearlescent samples because pearlescent pigments employed in automotive coatings are commonly mixed with metallic particles to integrate the two effects in one single paint. With regard to solid samples, the spectral reflectance, chroma, and luminance remained stable in the eight geometries with only minor fluctuations [Figs. 5(c) and 6(c)]

Figures 5(a), 5(b), 6(a), and 6(b) show that reflectance and lightness values, respectively, were higher at the geometries adjacent to the specular reflection (45° × : -60°, 45° × : -30°, 15° × : -30°, and 15° × :0°) and decreased drastically in the case of the furthest geometries. On the other hand, the most significant changes in the spectral profile emerged when comparing the measurements of geometries with the illuminant at different positions: 45° × : -60° and 45° × : -30° versus 15° × : -30° and 15° × :0°. These geometries are recommended for the evaluation of color change due to pearlescent pigments [8].

The following results are based on the average reflectance of the images for a more precise comparison with the BYK-mac and X-Rite MA98, since they do not offer pixel-wise reflectance data. At this stage, the spatially resolved images were not exploited because the main objective of this work was to perform a preliminary spectral and colorimetric validation of performance by means of comparing the new system against two commercial gonio-spectrophotometers. The next stage will focus on spatial features of goniochromatic pigments such as sparkle, graininess, and mottling under broad-band and narrow-band light sources. The deeper penetration of IR light will provide a more accurate analysis of the goniochromatic particles located at deeper layers of the coating and will also contribute to quantify their influence on the total appearance of the pigment. Preliminary results have revealed a better discrimination of some spatial attributes in the IR range due to the removal of sparkle at this spectral region and for coatings of different thickness.

A. Stability and Repeatability Performance

The results for stability assessments demonstrated excellent performance of all spectral channels with differences among repetitions below 5.75% for the UV-VIS camera and under 1.97% for the IR camera. The most outstanding shifts due to the influence of the sample positioning appeared when replacing it, but they were considered minor fluctuations because the deviation values never exceeded 4%.

Temporal noise analysis led to maximum differences below 1% when comparing the mean digital levels of the three sets of frames. This percentage was calculated with respect to the maximum digital level of each camera: 1023 for the UV-VIS and 16383 for the IR. The minimum number of frames (three) was selected for each acquisition.

The positioning repeatability evaluation of the rotation stages revealed a maximum positioning deviation under 1%, which confirmed the accuracy of both stages.

B. Spectral Performance in the Visible Range

The first data evaluated were the spectral reconstructions from 400 to 700 nm by means of the MAE, RMSE, and GFC. We should stress that the MAEs and the RMSEs are expressed as reflectance differences. These three metrics were computed for the three ROIs and the three pigment categories. The performance among ROIs was very similar and validated the use of the maximum measurement area without undermining the fitting; therefore, only the results for the full ROI are shown. Figure 7 plots the mean values considering the different geometries for the three types of samples; each bar includes the standard error as a measure of uncertainty.

The precise reconstructions obtained with the developed system revealed that all the mean values of MAE and RMSE were below 0.03 and very similar, which means that very few outliers were found. The mean GFCs, all above 0.9900, also proved the color accuracy. The GOHYLED system and the BYK-mac exhibited slightly more similar behavior than the X-Rite; in terms of MAE and RMSE this result was similar to the result of comparing the two commercial devices. With regard to the scale for the GFC, the evaluation of pearlescent and solid pigments can be considered "colorimetrically accurate" since the mean values of this parameter were above 0.9950, while metallic pigments attained "good spectral fitting" with values slightly above 0.9990. These last subsets of pigments also achieved correlations very similar to the correlations between the two gonio-spectrophotometers. In agreement with previous studies [36,37], the measurement geometries closer to the specular reflection (45° × : -60°, 45° × : -30°, 15° × :30°, and 15° × :0°) resulted in larger differences. At these geometries, the amount of light reflected is very high and any small variation in position or configuration can produce substantial deviations of the results.

Color differences again showed better correlations between the GOHYLED system and the BYK-mac, although the deviations with respect to the X-Rite MA98 were less noticeable than in the fitting metrics (Fig. 8). The greatest spectral and colorimetric match obtained for the GOHYLED system and the BYK-mac was probably due to the use of the same spectral filtering technique, i.e., LEDs, with similar spectral features such as the peak wavelength and the FWHM.

In general, the mean CIEDE2000 values were below 2 units with all instruments and for the three kinds of samples. These colorimetric differences remained within the ranges proposed in a previous study [38], where the authors suggested to widen color tolerances when using newer versions of standardized color-difference formulas such as the CIEDE2000; this study did not cover non-standard color-difference equations such as the AUDI2000. This tolerance proposal was based on the large numbers of factors that determine the reproduction of automotive coatings: add-on parts, closeness to the specular angle, $L^* > 100$, and visual texture. Considering all these circumstances, they recommended to apply a multiplication factor between 1.5 and 3 with respect to the visual discrimination threshold, traditionally equal to 1.

In contrast, the AUDI2000 color differences were larger, particularly for solid samples. It is known that this color-difference formula is stricter than the CIEDE2000, particularly for solid pigments, because their appearance is considered less complex and easier to reproduce than for goniochromatic pigments. Since the solid samples employed in this study

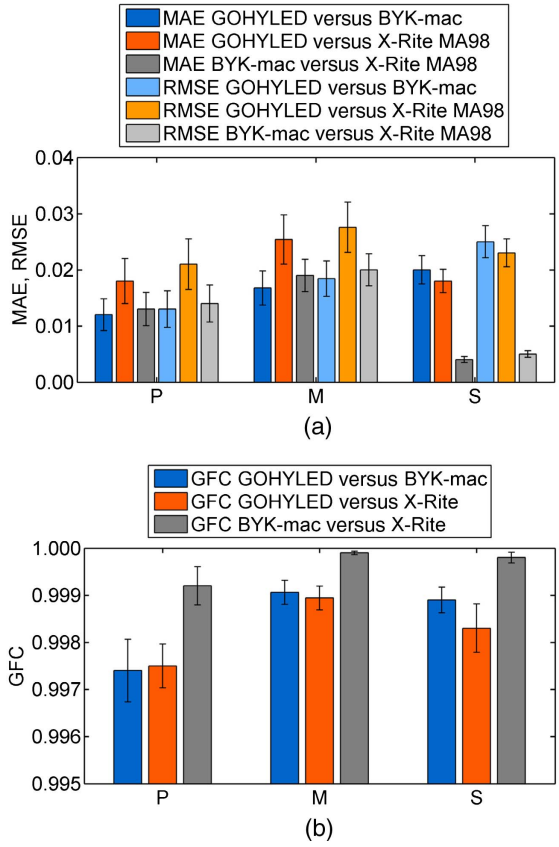

Fig. 7. Mean values of (a) MAEs and RMSEs and (b) GFCs for the spectral reconstruction of the GOHYLED system with respect to the BYK-mac and the X-Rite MA98 and the comparison between two gonio-spectrophotometers. The three metrics were plotted for pearlescent (P), metallic (M), and solid (S) samples. The error bars represent the standard error.

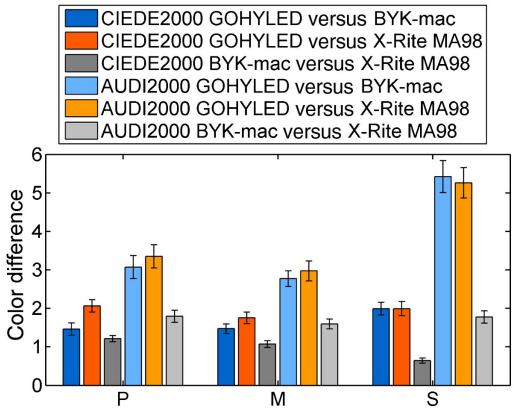

Fig. 8. Mean CIEDE2000 and AUDI2000 color differences of the GOHYLED system with respect to the BYK-mac and the X-Rite MA98 and also the comparison between the two gonio-spectrophotometers for the full ROI. Both metrics were plotted for pearlescent (P), metallic (M), and solid (S) samples. The error bars represent the standard error.

showed surfaces with more gloss than the pearlescent and metallic, any minor variation in the configuration could cause considerable variations among instruments. With regard to Fig. 8, the values shown were calculated considering the whole set of measurement geometries.

The comparisons with the GOHYLED system were very similar to the comparison between the two commercial gonio-spectrophotometers, especially for pearlescent and metallic pigments in terms of MAE, RMSE, and CIEDE2000. We can thus infer that the BYK-mac and X-Rite MA98 present differences of a magnitude similar to the GOHYLED. However, the correlation of their measurements for solid pigments was better than with the proposed instrument. Indeed, solid pigments showed a very glossy surface, to which the GOHYLED system seemed to be more sensitive than the gonio-spectrophotometers. Since the ROIs employed were the same as those of the commercial devices, the illumination path might be considered responsible for these differences. A collimated beam and/or a smaller aperture could increase the fitting with the reference devices. Finally, even though the correlations presented provide valuable information, further validation by means of psychophysical experiments is still needed.

C. Spectral Performance in the Infrared Range

Figure 9 shows the results of the validation of the IR range from 700 to 1309 nm. In this case, only the spectral fitting metrics (MAE, RMSE, and GFC) were computed. Besides the full ROI, the ROI of 12 mm was also analyzed, since it was the most appropriate according to the measurement area of the TOP 100 from the SPECTRO 320 spectrometer. Similarly to the performance in the VIS range, no remarkable differences were detected between the different ROIs in the IR range. Consequently, only the results related to the full ROI are shown.

These results also proved the good performance of the developed system in the IR range, although they were less accurate than in the VIS range due to the lower density of spectral bands, the greater spacing among them, and their wider FWHMs. Focusing on the results, the mean values of the MAEs and the RMSEs were below 0.07 and especially small in the case of the solid samples. The mean GFCs were above 0.9500, with the higher values obtained for the metallic samples just below 0.9950; therefore, the highest categories of the GFC scale were not reached in the IR. Results from the two ROIs revealed similar outcomes. Additionally, the geometries nearer to the specular reflection again caused the larger differences (45° × : -30°, 15° × :0°). Similarly, the values shown in Fig. 9 were calculated from the three measurement geometries.

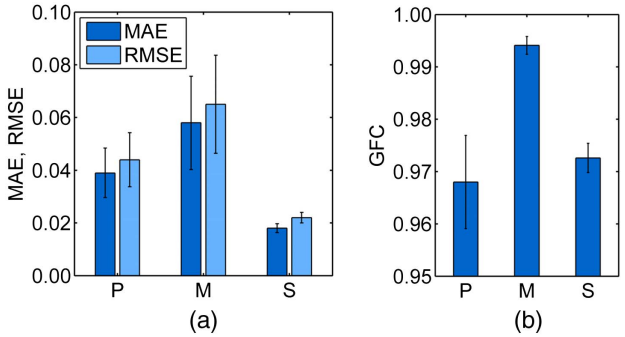

Fig. 9. Mean values of (a) MAEs and RMSEs and (b) GFCs for the spectral reconstruction of the GOHYLED system for the full ROI with respect to the SPECTRO 320. The three metrics were plotted for pearlescent (P), metallic (M), and solid (S) samples. The error bars represent the standard error.

Although the evaluation of goniochromatic pigments in the IR range is not common practice, it can provide useful spectral data on deeper layers of coatings, as well as additional information about visual effects that do not produce glint, such as graininess and mottling. Preliminary data obtained with the developed system have revealed that sparkling effects are extremely diminished in this region of the electromagnetic spectrum, and, therefore, they would not interfere with the assessment of other spatial phenomena such as those previously mentioned. For instance, IR light could also be used for the study of graininess instead of or in addition to diffuse VIS light.

5. CONCLUSIONS

A gonio-hyperspectral imaging system based on LEDs has been developed and validated for the analysis of automotive coatings. The design conforms to the standards DIN 6175-2, ASTM E2194, and ASTM E2539 for multi-angle color measurement of goniochromatic pigments.

The system provided precise reconstructions of spectral reflectances when compared to commercial devices in the IR (SPECTRO 320) and especially in the VIS range (BYK-mac and X-Rite). The differences would decrease if both spectral ranges had similar density of spectral bands, similar spectral steps, and similar FWHMs. Unfortunately, current solid-state technology does not provide LEDs above 800 nm with these features. Similarly, color differences were smaller compared with the BYK-mac, although deviations with respect to the X-Rite were lower than for the previous metrics. In general, the mean CIEDE2000 values were within recommended tolerance ranges and smaller than the higher values of the AUDI2000 due mainly to the solid pigments.

A thorough examination of the correlations obtained with the whole spectral range revealed that the different ROIs showed analogous results. Another shared outcome was that the most sensitive geometries were those closer to the specular reflection, 45° × : -60°, 45° × : -30°, 15° × : -30°, and 15° × :0° for the VIS and 45° × : -30° and 15° × :0° for the IR.

Lastly, one of the main advantages of the GOHYLED system is the inclusion of the spectral analysis in the two ranges of the electromagnetic spectrum, VIS and IR, and for all the measurement geometries recommended for the characterization of goniochromatic pigments [6–8]. Currently, the GOHYLED system is the only instrument with these attributes. Ongoing research focuses on the assessment of spatial effects such as sparkle, graininess, and mottling under white light and narrow-band light sources. The higher spatial resolution offered by the GOHYLED system in comparison with other instruments makes it particularly suitable for this task. Further studies will compare these results with those obtained by means of psychophysical experiments to accurately validate the performance of the GOHYLED system.

Funding. Ministerio de Ciencia e Innovación (MICINN) (DPI2011-30090-C02-01); European Union.

Acknowledgment. Francisco J. Burgos-Fernández thanks the Government of Catalonia for his Ph.D. grant.

REFERENCES

1. P. Bamfield, *Chromic Phenomena* (Royal Society of Chemistry, 2001).
2. F. J. Maile, G. Pfaff, and P. Reynders, "Effect pigments—past, present and future," Prog. Org. Coat. **54**, 150–163 (2005).
3. G. Pfaff, *Special Effect Pigments: Technical Basics and Applications*, 2nd ed. (William Andrew, 2008).
4. G. Buxbaum and G. Pfaff, *Industrial Inorganic Pigments*, 3rd ed. (Wiley-VCH, 2005).
5. E. Perales, E. Chorro, V. Viqueira, and F. M. Martínez-Verdú, "Reproducibility comparison among multiangle spectrophotometers," Color Res. Appl. **38**, 160–167 (2013).
6. "Tolerances for automotive paints—Part 2: Goniochromatic paints," DIN 6175-2 (DIN Deutsches Institut für Normung, 2001).
7. "Standard practice for multiangle color measurement of metal flake pigmented," ASTM Standard E2194-09 (ASTM International, 2009).
8. "Standard practice for multiangle color measurement of interference pigments," ASTM Standard E2539-08 (ASTM International, 2008).
9. A. M. Rabal, A. Ferrero, J. Campos, J. L. Fontecha, A. Pons, A. M. Rubiño, and A. Corróns, "Automatic gonio-spectrophotometer for the absolute measurement of the spectral BRDF at in- out-of-plane and retroreflection geometries," Metrologia **49**, 213–223 (2012).
10. H. Li, S. C. Foo, K. E. Torrance, and S. H. Westin, "Automated three-axis gonioreflectometer for computer graphics applications," Opt. Eng. **45**, 043605 (2006).
11. J. Liu, M. Noël, and J. Zwinkels, "Design and characterization of a versatile reference instrument for rapid, reproducible specular gloss measurements," Appl. Opt. **44**, 4631–4638 (2005).
12. M. E. Nadal and E. A. Thompson, "NIST reference goniophotometer for specular gloss measurements," J. Coat. Technol. **73**, 73–80 (2001).
13. D. Combes, I. Moya, S. Jacquemoud, and H. Sinoquet, "Un nouveau dispositif de mesure des propriétés optiques spectrales et bidirectionnelles de surfaces végétales (Thème n°4)," in *8th International Symposium Physical Measurements & Signatures in Remote Sensing*, Aussois, France, 2001, pp. 283–284.
14. H. Haneishi, T. Iwanami, N. Tsumura, and Y. Miyake, "Goniospectral imaging of 3D objects," in *Sixth Color Imaging Conference: Color Science, Systems and Applications*, Scottsdale, Arizona, 1998, pp. 173–176.
15. K. Tonsho, Y. Akao, N. Tsumura, and Y. Miyake, "Development of gonio-photometric imaging system for recording reflectance spectra of 3D objects," Proc. SPIE **4663**, 370–378 (2001).
16. T. Senzaki, Y. Harada, K. Ishikura, J. Hayashi, N. Tsumura, and Y. Miyake, "Development of gonio-spectral imaging software for highly accurate digital archive system," Jpn. Hardcopy **2002**, 490–491 (2002).
17. Y. Akao, N. Tsumura, P. G. Herzog, Y. Miyake, and B. Hill, "Gonio-spectral imaging of paper and cloth samples under oblique illumination conditions based on image fusion techniques," J. Imaging Sci. Technol. **48**, 227–234 (2004).
18. A. Kimachi, "Development and calibration of a gonio-spectral imaging system for measuring surface reflection," IEICE Trans. Inf. Syst. **E89-D**, 1994–2003 (2006).
19. E. Perales, E. Chorro, V. Viqueira, and F. M. Martínez-Verdú, "Reproducibility comparison among multiangle spectrophotometers," Color Res. Appl. **38**, 160–167 (2013).
20. D. B. Kim, M. K. Seo, K. Y. Kim, and K. H. Lee, "Acquisition and representation of pearlescent paints using an image-based gonio-spectrophotometer," Opt. Eng. **49**, 043604 (2010).
21. M. R. Pointer, N. J. Barnes, M. J. Shaw, and P. J. Clarke, "A new goniospectrophotometer for measuring gonio-apparent materials," Coloration Technol. **121**, 96–103 (2005).
22. H. Andrews and H. Hou, "Cubic splines for image interpolation and digital filtering," IEEE Trans. Acoust. Speech Signal Process. **26**, 508–517 (1978).
23. J. Kiusalaas, *Numerical Methods in Engineering with MATLAB* (Cambridge University, 2005).
24. A. Kurekin, V. Lukin, A. Zelensky, P. Koivisto, J. Astola, and K. Saarinen, "Comparison of component and vector filter performance with application to multichannel and color image processing," in *IEEE-EURASIP Workshop on Nonlinear Signal and Image Processing (NSIP)*, Antalya, Turkey, 1999, pp. 38–42.
25. J. Farifteh, F. Van der Meer, C. Atzberger, and E. J. M. Carranza, "Quantitative analysis of salt-affected soil reflectance spectra: a comparison of two adaptive methods (PLSR and ANN)," Remote Sens. Environ. **110**, 59–78 (2007).
26. F. H. Imai, M. R. Rosen, and R. S. Berns, "Comparative study of metrics for spectral match quality," in *The First European Conference on Colour Graphics, Imaging, and Vision*, Poitiers, France, 2002, pp. 492–496.
27. J. Hernández-Andrés, J. Romero, and R. L. Lee, "Colorimetric and spectroradiometric characteristics of narrow-field-of-view clear skylight in Granada, Spain," J. Opt. Soc. Am. A **18**, 412–420 (2001).
28. J. Herrera-Ramirez, M. Vilaseca, F. J. Burgos, L. Font, R. Senserrich, and J. Pujol, "Artwork imaging from 370 to 1630 nm using a novel multispectral system based on light-emitting diodes," Color Res. Appl. **40**, 398–407 (2015).
29. J. Schanda, *Colorimetry: Understanding the CIE System* (Wiley, 2007).
30. N. Ohta and A. R. Robertson, *Colorimetry: Fundamentals and Applications* (Wiley, 2005).
31. M. R. Luo, G. Cui, and B. Rigg, "The development of the CIE 2000 colour-difference formula: CIEDE2000," Color Res. Appl. **26**, 340–350 (2001).
32. Commission Internationale de l'Éclairage, "Improvement to industrial colour-difference evaluation," Tech. rep. CIE 142-2001 (CIE Central Bureau, 2001).
33. T. Dauser, "Audi color tolerance formulas," Tech. rep. (AUDI AG, 2012).
34. P. Capilla, J. Artigas, and J. Pujol, *Fundamentos de colorimetría* (Universitat de València, 2002).
35. M. Melgosa, A. Trémeau, and G. Cui, "Colour difference evaluation," in *Advanced Color Image Processing and Analysis* (Springer, 2013), pp. 65–85.
36. E. Chorro, E. Perales, F. J. Burgos, O. Gómez, M. Vilaseca, V. Viqueira, J. Pujol, and F. M. Martínez-Verdú, "The minimum number of measurements for colour, sparkle, and graininess characterisation in gonio-apparent panels," Coloration Technol. **131**, 303–309 (2015).
37. N. Dekker, E. J. J. Kirchner, R. Supèr, G. J. van den Kieboom, and R. Gottenbos, "Total appearance differences for metallic and pearlescent materials: contributions from color and texture," Color Res. Appl. **36**, 4–14 (2011).
38. E. J. J. Kirchner and J. Ravi, "Setting tolerances on color and texture for automotive coatings," Color Res. Appl. **39**, 88–98 (2014).